

(ii) the energy diffuses according to the diffusion equation with no time variation of the thermal diffusion constant, (iii) the pump mechanism is collisional and varies directly as molecular velocity and thus as the square root of temperature, and (iv) the maser is saturated—that is, the principal relaxation from the upper masering level is through induced maser transitions. The result of the calculation is given by the solid curve in Fig. 2, which fits the data very well throughout the observing sequence. Only the time scale (that is, the thermal diffusion constant) is varied in the model; otherwise there are no free parameters. Other models have been tried, including a heat pulse of length comparable to the diffusion time and a heat pulse with radiational pumping. None of these models give as satisfactory a fit to the data.

The quantitative requirements of the model seem reasonable. If one postulates an O5 star with  $L = 8 \times 10^5 L_{\odot}$  and an ionized cavity 100 A.U. in radius, and the break in the cocoon grows for 1 day at a velocity of 1 km/sec and then heals at the same rate, the heat pulse would be sufficiently short. The supply of energy would be equal to the observed luminosity change (assuming an isotropic maser). It is interesting to note that the maser would be the principal exit channel for the energy in the heat pulse, since the shorter-wavelength radiation propagates too slowly to escape until the temperature drops below 200°K. The characteristic time of the observed variation is consistent with such a model, since the maser dimension is  $10^{13}$  to  $10^{15}$  cm, depending on the ratio of observed size to true size. A shock wave with a velocity of 10 km/sec would require months to years to traverse the region, while radiation traveling unimpeded would require  $10^3$  to  $10^5$  seconds, which is too fast. Thus, diffusion of radiation is more consistent with the observed time scale. The cocoon model for W3 (OH) itself does have difficulties, as Forster *et al.* (9) have pointed out. Not enough infrared radiation seems to be coming from the proposed cocoon star. The calculated curve shown in Fig. 2 does not depend on the cocoon star model, of course, since any pulsed source of energy would serve.

A. D. HASCHICK, B. F. BURKE  
Research Laboratory of Electronics,  
Department of Physics,  
Massachusetts Institute of Technology,  
Cambridge 02139

J. H. SPENCER  
E. O. Hulburt Center for Space  
Research, Naval Research Laboratory,  
Washington, D.C. 20375

## References and Notes

1. J. M. Moran, B. F. Burke, A. H. Barrett, A. E. Rogers, J. A. Ball, J. C. Carter, D. D. Cuda-back, *Astrophys. J. Lett.* **152**, L97 (1968); B. F. Burke, D. C. Papa, G. D. Papadopoulos, P. R. Schwartz, S. H. Knowles, W. T. Sullivan, M. L. Meeks, J. M. Moran, *ibid.* **160**, L63 (1970). See also reviews by B. F. Burke [*Int. Astron. Union Symp.* **60** (1975), p. 252] and J. M. Moran [*Frontiers of Astrophysics*, E. Avrett, Ed. (Harvard Univ. Press, Cambridge, 1976), p. 385].
2. P. Goldreich and D. A. Keely, *Astrophys. J.* **174**, 517 (1972); M. M. Litvak, *ibid.* **182**, 711 (1973).
3. D. Buhl, L. E. Snyder, P. R. Schwartz, A. H. Barrett, *Astrophys. J. Lett.* **158**, L97 (1969); W. T. Sullivan III, *ibid.* **166**, 321 (1971); R. H. Gammon, *Astron. Astrophys.* **50**, 71 (1976).
4. J. M. Moran *et al.*, *Astrophys. J.* **185**, 535 (1973).
5. J. M. Bologna, K. J. Johnston, S. H. Knowles, S. A. Mango, R. M. Sloanaker, *ibid.* **199**, 86 (1975).
6. C. G. Wynn-Williams and E. E. Becklin, *Publ. Astron. Soc. Pac.* **86**, 5 (1974); R. L. Brown and

B. Zuckermann, *Astrophys. J. Lett.* **202**, L125 (1975).

7. M. M. Litvak, *Science* **165**, 855 (1969); P. Goldreich and J. Kwan, *Astrophys. J.* **191**, 93 (1974).
8. T. de Jong, *Astron. Astrophys.* **26**, 297 (1973).
9. J. R. Forster, W. J. Welch, M. C. H. Wright, *Astrophys. J. Lett.* **215**, L121 (1977).
10. We thank all those who sacrificed observing time or helped obtain spectra in order to fill up gaps in the data. These include W. Dent, P. Ho, K. J. Johnston, S. E. Kleinmann, T. Balonek, N. Cohen, J. Garcia-Barreto, P. Greenfield, M. Schneps, P. Solomon, J. M. Bologna, C. H. Mayer, and N. J. Santini. Special thanks are due to T. Giuffrida, who contributed a major block of observing time and supervised many observations at the Haystack Observatory. Thanks are also due to the Haystack staff and operators who assisted in the observations and helped obtain extra observing time. This research was supported by a grant from the National Science Foundation. The Haystack Observatory of the Northeast Observatory Corporation is supported by the National Science Foundation.

9 August 1977; revised 12 September 1977

## Hominoid Enamel Prism Patterns

**Abstract.** *Analysis of enamel prism patterns in a selected series of extant hominoids reveals that pongids have a pattern distinctively different from that of Homo sapiens. The pattern for a Miocene hominoid, Ramapithecus, is very similar to that seen in Homo sapiens. The finding allows a new approach to the evaluation of isolated teeth.*

Teeth are often the most abundant, and frequently the only, remains of fossil primates found; thus it is essential that every piece of information from these particularly indestructible structures be evaluated. At present, most of our knowledge of Miocene hominoids, including possible ancestors of later hominids, is based on dental remains. Correct interpretation of these remains is crucial to understanding hominid phylogeny, and this is especially true when isolated remains are analyzed. Data obtained from these specimens have often led to a variety of conflicting interpretations. Morphological analysis of occlusal surfaces, especially when isolated teeth are evaluated, may not provide definitive answers regarding either adaptation or phylogeny. For a more adequate appraisal additional analytic methods and techniques must be used. Scanning electron microscopy of enamel prism patterns is one such technique.

The study of enamel prism patterns is not new. Tomes (1) was the first to attempt an analysis of the structure of enamel as a possible taxonomic character in the marsupials. Later, Carter (2) applied Tomes's techniques to the study of a series of primates, including a number of fossil prosimians. The data obtained from the study by Carter led Regan (3) to devise a new classification of the order Primates. However, these studies were not well received by other researchers and had little, if any, effect on classification or theories of primate evolution.

The reason for this was, perhaps, a lack of understanding of the ultrastructure of enamel in man and other mammals.

It was not until the advent of the scanning electron microscope (SEM) that researchers could begin to understand the development and ultrastructural features of enamel, especially the enamel prism. The work of Boyde (4) has done much to provide a more comprehensive understanding of enamel structure in mammals. Analyses with the SEM of developing and mature enamel have documented the fact that specific enamel prism patterns do exist and can be used as a taxonomic indicator (4). The purpose of the research reported here was to develop a nondestructive method of analysis to evaluate the enamel of primates, with emphasis on studying isolated teeth. The work of Carter (2), Shobusawa (5), and Boyde (4, 6) provided data which indicated that a study of the enamel prism patterns could yield reproducible results. Therefore, a study was conducted to determine the enamel prism patterns in a select sample of primate teeth, with emphasis on Hominoidea.

Molar and premolar teeth were obtained from a number of extant and extinct primates. These specimens were cleaned in absolute alcohol and acetone for 1 hour each and were then etched in a 10 percent solution of hydrochloric acid for 2.5 minutes. This procedure usually removed the outer, prismless layer. The specimens were subsequently washed in

two baths of distilled water and air-dried for 1 hour.

The specimens were then glued to aluminum stubs with a silver conductive compound and air-dried. The whole tooth was mounted with either the buccal or the lingual surface of the cervical crown facing the electron beam. The mounted specimens were coated with about 100 Å of carbon and about 150 Å of gold by the methods outlined by Boyde (6). This procedure ensures complete coverage of the specimen to provide an even conductive coating.

The specimens were examined in an AMR-900 scanning electron microscope at various magnifications. Photographs were taken to provide a permanent record of the enamel prism patterns. The critical factor in the analysis of prism patterns is the determination of the direction of the crystallites within the prisms and the direction of the prisms

with respect to the plane of view (7). This was accomplished by rotating the specimen so that the heads of the prisms were perpendicular to the electron beam. In this way, duplication of results was obtained for all the specimens studied.

The enamel prism pattern in *Homo sapiens* is well documented and has been described as a keyhole pattern (8). Analysis of the enamel prism pattern of *H. sapiens*, using the methods described above, confirmed the existence of the keyhole pattern (Fig. 1). The sample of pongids consisted of teeth from five individuals for each of the species *Pan troglodytes*, *Gorilla gorilla*, and *Pongo pygmaeus*. The analysis revealed that the enamel prism pattern was either circular or hexagonal (Fig. 2). Identical patterns were observed within and between species.

A fossil hominoid specimen from the Chinji Formation of the Siwalik Group in

Pakistan was analyzed by the methods described above. The specimen, AMNH 19565-B, is an unworn right lower molar ( $M_1$ ) of *Ramapithecus punjabicus*. It was collected in 1922 by Barnum Brown's expedition but was unrecognized until 1974. Analysis of the specimen showed a pattern very similar to the keyhole pattern described in man (Fig. 3). A second etching and subsequent analysis of the specimen did not reveal a circular or hexagonal pattern as found in the pongids. The empty appearance of the keyholes is due to the fossilized state of the tooth and the effect of differential etching.

Thus, the analysis of enamel prism patterns showed a circular pattern for the pongids (Fig. 2), which can be easily differentiated from the keyhole pattern observed in *H. sapiens* (Fig. 1). Subsequent analysis of an isolated fossil tooth, identified as belonging to the tax-

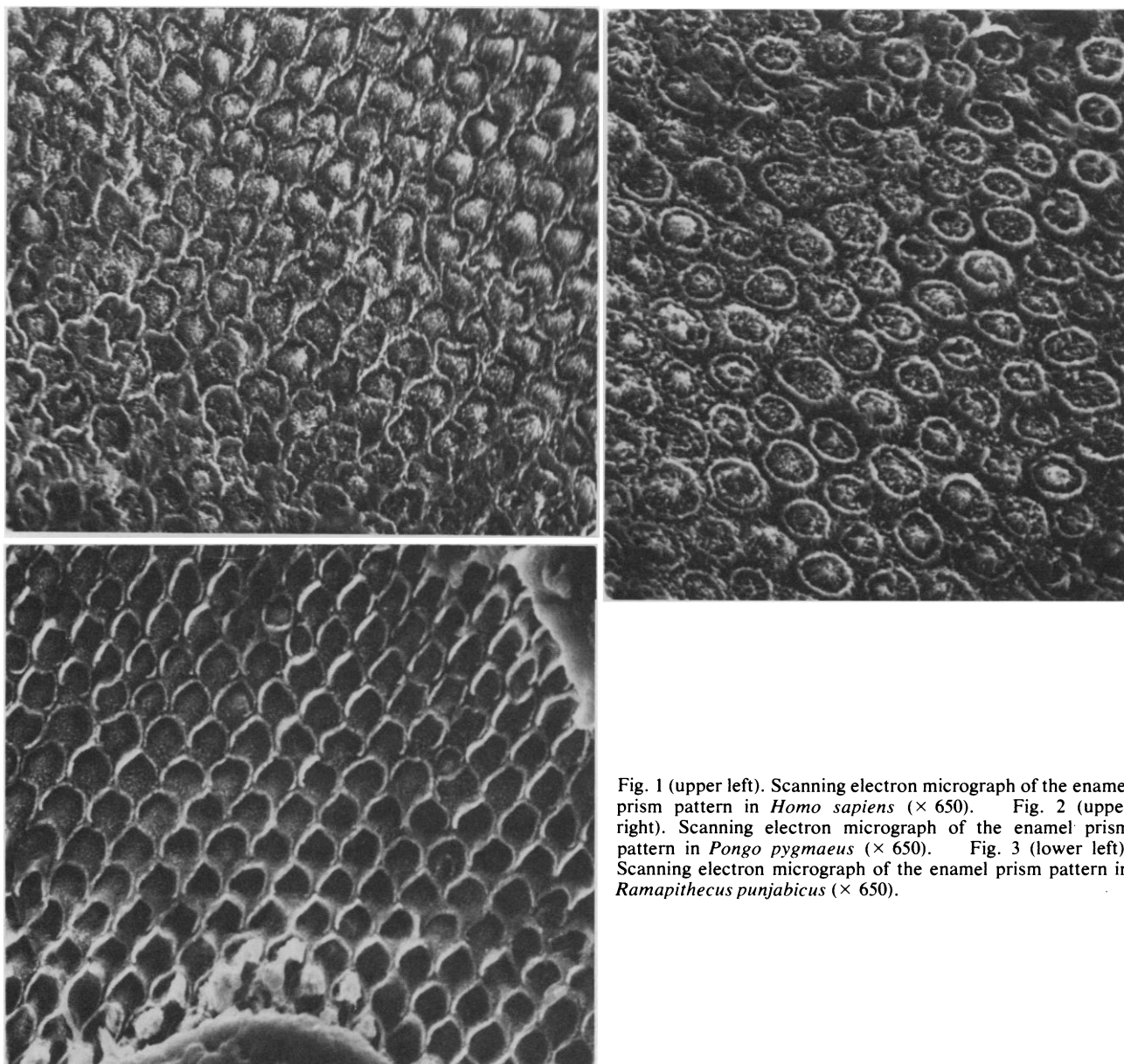


Fig. 1 (upper left). Scanning electron micrograph of the enamel prism pattern in *Homo sapiens* ( $\times 650$ ). Fig. 2 (upper right). Scanning electron micrograph of the enamel prism pattern in *Pongo pygmaeus* ( $\times 650$ ). Fig. 3 (lower left). Scanning electron micrograph of the enamel prism pattern in *Ramapithecus punjabicus* ( $\times 650$ ).

on *R. punjabicus*, revealed that the enamel prism pattern is very similar to that of *H. sapiens*.

Interpretation of these structural differences is at present conjectural. The differences in prism packing between living pongids and hominids may be correlated with differences in enamel thickness, pongids having thin enamel while hominids have thick enamel (9). The *Ramapithecus* molar exhibits thick enamel and a hominid-like prism pattern. However, before drawing any conclusions about phylogeny (that is, whether *Ramapithecus* is ancestral to later hominids), it will be necessary both to examine a full range of extinct Neogene hominoids and to analyze the functional significance of prism packing and enamel thickness (10).

The patterns obtained are reproducible, and the method used is non-destructive. Prism patterns appear to be potentially very interesting for functional analysis and, perhaps, eventually for phylogenetic and taxonomic purposes.

DAVID G. GANTT\*

Department of Anthropology,  
Washington University,  
St. Louis, Missouri 63130

DAVID PILBEAM

Department of Anthropology,  
Yale University,  
New Haven, Connecticut 06520

GREGORY P. STEWARD

Department of Anatomy, School of  
Dental Medicine, Southern Illinois  
University, Alton 62002

#### References and Notes

1. J. Tomes, *Philos. Trans. R. Soc. London* **139**, 403 (1849).
2. J. T. Carter, *J. Anat.* **54**, 189 (1920); *Proc. Zool. Soc. London* (1922), p. 599.
3. C. T. Regan, *Ann. Mag. Nat. Hist. London* **6**, 383 (1930); *Nature (London)* **125**, 125 (1930).
4. A. Boyde, thesis, University of London (1964); in *Tooth Enamel*, R. W. Fearnhead and M. V. Stack, Eds. (Wright, Bristol, England, 1965), pp. 163-167; in *Calcified Tissues*, H. Fleish, J. J. Blackwood, M. Owen, Eds. (Springer-Verlag, New York, 1966), pp. 276-280; in *Dental Morphology and Evolution*, A. A. Dahlberg, Ed. (Univ. of Chicago Press, Chicago, 1971), pp. 81-93.
5. M. Shobusawa, *Okajimas Folia Anat. Jpn.* **24**, 371 (1952).
6. A. Boyde, *Proc. R. Soc. Med.* **60**, 13 (1967); *Bull. Group. Int. Rech. Sci. Stomatol.* **12**, 151 (1969); *Z. Zellforsch. Mikrosk. Anat.* **93**, 583 (1969).
7. J. W. Osborn, *Oral Sci. Rev.* **3**, 1 (1974).
8. A. H. Meckel, in *Chemistry and Physiology of Enamel* (Univ. of Michigan Press, Ann Arbor, 1971), pp. 25-42.
9. D. G. Gantt, thesis, Washington University (1977); S. Molnar and D. G. Gantt, *Am. J. Phys. Anthropol.* **46**, 447 (1977); E. L. Simons, *Sci. Am.* **236**, 28 (May 1977); — and D. Pilbeam, in *Functional and Evolutionary Biology of Primates*, R. H. Tuttle, Ed. (Aldine, Chicago, 1972), pp. 36-62.
10. D. G. Gantt and D. Pilbeam, in preparation.
11. We thank M. L. Heager and M. Veith for technical assistance and M. C. McKenna for allowing us access to the *Ramapithecus* specimen. This research was in part supported by NSF grants 75-23306 BMS, GS-36482, and SOC 75-19191.

\* Present address: Department of Anthropology, Florida State University, Tallahassee 32306.

## Fascioliasis: Role of Proline in Bile Duct Hyperplasia

**Abstract.** In animals with fascioliasis, extensive hyperplasia of the main bile duct occurs that often results in enlargement of the duct to more than 20 times the normal. We report that proline infused into the abdominal cavity of rats caused hyperplasia of the bile duct resembling that produced in the early stages of the disease. We suggest that *Fasciola hepatica*, which synthesizes and releases large amounts of proline, induces enlargement of the bile duct by a similar mechanism.

*Fasciola* and several other fluke genera, among them *Dicrocoelium*, *Clonorchis*, and *Opisthorchis*, cause liver fluke disease. Every year thousands of cases of this disease are reported in humans, and losses from infected livestock total millions of dollars. Regardless of the host or fluke genus causing liver fluke disease, the pathology includes a usually striking enlargement of the main bile duct (1). The enlargement is due to cellular proliferation or hyperplasia that results in a thickened duct wall and a much infolded endothelium surrounding the enlarged duct lumen. This process is probably essential to the establishment of the disease, particularly for those flukes (including the genera given above) that inhabit the bile duct, because the normal bile duct is too narrow to accommodate the worms, which are of a relatively large size. Furthermore, the proliferated endothelium in the duct may provide an important source of nourishment to the worms (2, 3).

Because hyperplasia of the main bile duct occurs while immature *Fasciola* are still in the liver parenchyma and long before they actually enter the duct, Dawes (3) suggested that the hyperplasia was induced by chemical rather than mechanical stimulation. This hypothesis was confirmed in our laboratory by using *Fasciola* implanted into the peritoneal cavity of rats (4). Hyperplasia of the bile duct occurred even though the worms were implanted only in the peritoneal cavity and were encased in a nylon mesh sack that precluded their direct contact with the liver or bile duct. This study also showed that the testing of various substances to determine their potential as inducers of the hyperplasia of fascioliasis could be greatly simplified. Introduction of the inducing agent directly into the bile duct or liver was not neces-

sary because the inducer was effective from the peritoneal cavity. Hence the current investigation was based on this observation. In experiments in which test substances were pumped into the peritoneal cavity of rats we found that the amino acid proline may be the active agent inducing the bile duct hyperplasia of fascioliasis, a finding that could have broad implications not only for understanding a key element in the establishment of liver fluke symbiosis but also in the areas of morphogenetic regulation and tumor growth.

Proline is a major component of the free amino acid pool in bile fluid where its concentration increases by more than 10,000 times during infection by *Fasciola* (5). The production of this proline by the parasite is also indicated by the presence within the body of the worm of high concentrations of free proline (6) and of proline biosynthetic enzymes which show four to ten times the activity of their mammalian analogs (7).

The role of proline in inducing hyperplasia of the bile duct was suggested by several observations. First, proline concentrations in bile from host animals showed a fourfold increase by day 25 of infection, which was more than a month before the flukes entered the bile ducts. Although there was some increase in the other amino acids in the bile fluid, this was minor compared to the increase in proline and was not measurably different from normal until the worms actually entered the duct (5). Second, the bile duct tissue is rich in collagen whose biosynthesis is stimulated by increased levels of proline (8). Third, it is generally believed that bile duct hyperplasia occurs after stimulation of collagen synthesis (9), although a causal relation between the two effects apparently has not been documented.

Table 1. Comparison of luminal perimeters of bile ducts from rats treated with saline, proline, or a mixture of amino acids. The data are for two experiments (A and B) and are expressed as means  $\pm$  standard deviation.

Group	Treatment	Perimeter (mm)	
		A	B
1	Saline	2.03 $\pm$ 0.712	2.26 $\pm$ 0.796
2	Proline	2.94 $\pm$ 0.603	3.79 $\pm$ 1.421
3	Amino acid mixture	2.01 $\pm$ 0.519	2.12 $\pm$ 0.353
Significance		F (2, 18) > .025	F (2, 18) >> .01